Andrographolide attenuates RSV-induced inflammation by suppressing apoptosis and promoting pyroptosis after respiratory syncytial virus infection in vitro

Siyi Che
Chongqing Medical University Affiliated Children's Hospital
Xiaohong Xie
Chongqing Medical University Affiliated Children's Hospital
Jilei Lin
Shanghai Children's Medical Center Affiliated to Shanghai Jiaotong University School of Medicine
Ying Liu
Ganzhou Hospital of Traditional Chinese Medicine
Jun Xie
cyxiejun@126.com

Chongqing Medical University Affiliated Children's Hospital https://orcid.org/0000-0003-4122-5129
Enmei Liu
Chongqing Medical University Affiliated Children's Hospital

Research Article

Keywords: andrographolide, respiratory syncytial virus, network pharmacology, apoptosis, pyroptosis

Posted Date: March 15th, 2022

DOI: https://doi.org/10.21203/rs.3.rs-1422101/v1

Version of Record: A version of this preprint was published at Combinatorial Chemistry & High Throughput Screening on November 7th, 2023. See the published version at https://doi.org/10.2174/0113862073256465231024075452.

Abstract

Respiratory syncytial virus (RSV), the most common viral pathogen causing acute lower respiratory tract infection among children under five years old worldwide, still lacks specific therapeutic drugs. Andrographolide has been found efficacious in various virus infections, however, its effects on RSV infection remains unknown. Herein, in this study we quantified RSV virus load, IL-6 and IL-8 in A549 cell supernatant, and found andrographolide decreased the viral load and attenuated RSV-induced inflammation. Then, using online databases, we discovered 25 potential targets of andrographolide in the treatment of RSV-infected airway epithelial cells. Subsequently, GO and KEGG enrichment analysis led to the identification of CASP1, CCL5, JAK2, STAT1 as significant players. We verified the mRNA expression change of the potential target genes, which showed that andrographolide noticeably suppressed the increase of CASP1, CCL5, JAK2 and STAT1 post RSV infection. IL-1β, which is downstream of CASP1, was also up-regulated after RSV infection and down-regulated by andrographolide. Furthermore, we conducted Annexin V-FITC/PI apoptosis assay and Western blotting to determine whether andrographolide has an impact on the death pattern of RSV-infected cells. Interestingly, RSV infection decreased the protein levels of caspase-1, cleaved caspase-1, cleaved IL-1β, N terminal of GSDMD and Bcl-2, while andrographolide elevated them. These results suggested that andrographolide might attenuate RSV-induced inflammation by suppressing apoptosis and promoting pyroptosis of infected epithelial cells and thus inducing effective viral clearance.

Introduction

Respiratory syncytial virus (RSV) is a negative-sense single-strand RNA virus and the most common viral pathogen that causes acute lower respiratory tract infection worldwide among children under five years old[42]. Severe RSV infection in early childhood is closely related to recurrent wheezing and abnormal pulmonary function later in life[36]. The efficacy of Palivizumab, the only FDA-approved monoclonal antibody for prophylactic clinical application in RSV disease, remains limited[2]. Ribavirin, an anti-viral drug, used to treat virus infection, also exhibits considerable side effects[33]. Overall, despite its high incidence and economic burden that it imposes on the society, there is currently no specific therapeutic drug or reliable preventive vaccine against the RSV disease[51].

With long history, traditional medicine or alternative medicine has its unique and perspective advantages. Natural products have played pivotal roles in the drug discovery and development process, and have been widely applicated to treat a variety of diseases. *Andrographis paniculata* (Burm.f.) Nees, which belongs to the family Acanthaceae, is an annual herbaceous plant, native to India and Sri Lanka, but widely cultivated in Southeastern Asia[4]. It has long been used in traditional medicine to treat fever, dysentery, malaria, diabetes, snake bites, respiratory diseases, skin infections, urinary tract infections and so on since its discovery in 1951[19] [53] [1] [48] [13]. Diterpene lactones, flavonoids, and polyphenols are main bioactive compounds extracted from *Andrographis paniculata* (AP)[5]. Diterpene lactones such as andrographolide (AD), 14-deoxy-11,12-didehydroandrographolide (DDAD), and neoandrographolide (NAD) are reported as major components to exert the therapeutic properties of AP[38].

In Asian countries, including China, andrographolide has been successfully used to cure respiratory infection[21]. Among its multi-pharmacological effects, andrographolide has been found to exert antiviral function over a variety of viruses, such as influenza A virus[10] and ZIKA virus[22]. Since 2020, new attention has been drawn to andrographolide and its therapeutic advantage has been re-estimated due to their beneficial role in the combat against COVID-19 [43]. However, despite the wide clinical application of andrographolide in viral infection, there are few relevant research focusing on its effects and mechanism on RSV infection so far.

Traditional or alternative medicines did not become widely accepted due to unclear mechanisms of action. With the rapid development of bioinformatics and systematic biology, network pharmacology has been recognized as a highly effective method that has been successfully used to predict the multiple targets and mechanisms of traditional medicines in numerous diseases[17]. The present study, therefore, designed to firstly identify whether andrographolide has antiviral effect on RSV infection in vitro. Then aimed to analyze the potential targets of andrographolide for the treatment of RSV infection using online databases, and conducted in vitro experiments to uncover the underlying mechanisms.

Materials And Methods

Reagent, Cell Lines, and Virus preparation

Andrographolide was purchased from APExBIO (N1855, APExBIO, USA, purity 99.67%), with High Performance Liquid Chromatography (HPLC) and Nuclear Magnetic Resonance (NMR) reported quality control. Dimethyl sulfoxide (DMSO) was purchased (Solarbio, China). The Human lung carcinoma epithelial cell line A549 (CCL-185), and the human laryngeal cancer epithelial cell line HEp-2 (CCL-23) was obtained from the American Type Culture Collection (ATCC, USA), with Short Tandem Repeat (STR) authentication. Cells were screened to exclude from Mycoplasma contamination using a Mycoplasma Detection Kit (Yise Med, China). RSV-A2 strain (VR-1540, ATCC, USA) was grown in HEp-2 cells and purified by density gradient[14]. The virus titer of used RSV was 1.5 *10^8 PFU/ml, determined by serial dilution plaque assay as previously described[30].

Cell Counting Kit-8

To investigate whether andrographolide induces cytotoxicity, A549 cells were seeded in 96-well plates at a density of 3×10^4/mL and pre-incubated with Dulbecco's modified Eagle's medium (DMEM) (Gibco, USA) supplemented with 10% Fetal Bovine Serum (FBS) (AusgeneX, Australia) at 37^{o}C and 5% CO_2 overnight. Then cells were incubated with medium containing a serial concentration of andrographolide (5, 10, 20, 40, 80 μM) for 36 h. Wells without cells were set as blank, while cells incubated with 10% FBS culture medium were employed as control. After incubation, each well was replaced with 100μL medium supplemented with 10% CCK-8 reagent (Dojindo, Japan) and incubated for 2 h. Absorbance at 450 nm were detected using microplate reader and cell viability was calculated.

Cell culture and RSV infection

A549 was cultured and passaged in DMEM supplemented with 10% FBS at 37^{o}C and 5% CO_2. For RSV infection, the cells were seeded in 12- or 6-well plates at a density of 3×10^5/mL overnight. When the monolayer cell density reached ~ 80%, RSV A2 was added at a multiplicity of infection of 1. After incubation for 2 h, the culture medium was replaced with DMEM containing 2% FBS. Where used, 5 μM or 10 μM andrographolide or the same DMSO were added to the culture medium.

RNA isolation and RT-qPCR

After incubation for 24 h and 36 h, total A549 cells infected with RSV or not in 12-well plates were washed twice with phosphate buffer saline (PBS). RNA was extracted using RNAiso Plus reagent (TaKaRa, Japan) according to the manufacturer's instructions. RNA concentration and A260/A280 ratio were detected using NanoDrop™ One/One^C (Thermo Scientific, USA), and 1.0 μg of the RNA was reversely transcribed using a TaKaRa kit (TaKaRa, Japan). RSV N gene load was also quantified using TaqMan (TaqMan, USA) qPCR as previously described[9], and the qPCR cycle conditions were as follows: 50°C for 2 min, 95°C for 10 min, 40 cycles of 95°C for 15 s and 60°C for 1 min. The mRNA levels of target genes on each sample were measured and calculated according to the $2^{-\Delta\Delta Ct}$ method. GAPDH expression was quantified in all samples as reference. The primer sequences are shown in Table 1. The reaction conditions of qPCR were as follows: 95°C for 5 min, then a total of 40 cycles of 95°C for 10 s, 59°C for 15 s, and 72°C for 1 min.

Table 1
Target gene primer sequence

Genes	Forward (5'-3')	Reverse (3'-5')
Caspase-1	GCTGAGGTTGACATCACAGGCA	TGCTGTCAGAGGTCTTGTGCTC
CCL-5	CCTGCTGCTTTGCCTACATTGC	ACACACTTGGCGGTTCTTTCGG
JAK2	CCAGATGGAAACTGTTCGCTCAG	GAGGTTGGTACATCAGAAACACC
STAT1	TGTATGCCATCCTCGAGAGC	AGACATCCTGCCACCTTGTG
IL-1β	AAATACCTGTGGCCTTGGGC	TTTGGGATCTACACTCTCCAGCT
RSV-N	AGATCAACTTCTGTCATCCAGCAA	TTCTGCACATCATAATTAGGAGTATCAAT
GAPDH	ATCAAGAAGGTGGTGAAGCAGGC	TCAAAGGTGGAGGAGTGGGTGTC

Cell supernatant collection and Cytokine levels measurement

After incubation for 36 h, cell supernatants were collected after centrifuging at 3000 rpm for 5 min at 4^{o}C. Human IL-6 and IL-8 enzyme-linked immunosorbent assay (ELISA) (NEOBIOSCIENCE, China) was used to detect cytokine levels.

Identification of RSV infection-related genes

RNAseq dataset GSE32139 was downloaded from the Gene Expression Omnibus (GEO) database(https://www.ncbi.nlm.nih.gov/geo/). Human primary airway epithelial cells were harvested and cultured in a polarized system, and then infected with RSV. For the gene expression profile in GEO, the raw data were downloaded and normalized by the robust multiarray averaging method. Missing values were detected and omitted. The probes were then converted into the corresponding gene symbols according to the platform of mRNA dataset. The log value of each expression was adjusted by its mean and auto-scaled by its standard deviation. We defined $P < 0.05$ and $|logFC| > 0.05$ as cutoff values for screening the differentially expressed genes (DEGs). The “DESeq2” package of R software was used to analyze differentially expressed gene sets.

Identification of andrographolide-related genes

The chemical structure of andrographolide was downloaded from the PubChem website (https://pubchem.ncbi.nlm.nih.gov/), and imported to the PharmMapper Database (http://www.lilab-ecust.cn/pharmmapper/) to retrieve the predicted target proteins. PharmMapper Database is a free online reverse-docking database for potential target identification of small molecules using the pharmacophore mapping approach[49]. The gene names of target proteins were extracted from the website of UniProt Knowledgebase (http://www.uniprot.org).

GO and KEGG pathway enrichment analysis

The RSV infection-related and the andrographolide-related genes were merged and uploaded to the online Venn diagram package (http://bioinfogp.cnb.csic.es/tools/venny/index.html) for mapping. The intersection of the two parts was considered as the potential targets of andrographolide for the treatment of RSV infection. The “cluster Profiler” package of R software was used to conduct GO, KEEG analysis of the intersected genes.

Flow cytometry analysis

Following RSV infection in 6-well plates, A549 cells were incubated with culture medium or andrographolide (5μM, 10μM) for 36 h. Cell death was measured using the Annexin V-FITC/PI apoptosis assay kit (NEOBIOSCIENCE, China) according to the manufacturer’s instructions. Viable and apoptotic cells were differentiated and characterized by quadrant separation. The Annexin V+, PI- cells were considered as early apoptosis, and the Annexin V+, PI + cells as late apoptosis /necrosis[46]. The results were presented as mean percentage ratio of five biological replicates.

Western blot (Immunoblot) analysis

Following RSV infection for 36 h, total A549 cells in 6-well plates were washed twice with PBS, then harvested and lysed using RIPA buffer (CST, USA) containing PMSF (CST, USA) on ice. Lysates were centrifuged at 14,000 g for 10 min at 4^{o}C to obtain the supernatants. Samples containing equal quantities of protein were resolved in 10% SDS-PAGE and then transferred onto PVDF membranes

(MERCK MILLIOPORE, Germany). The membranes were blocked with 5% BSA for 1 h and probed with primary antibodies against Caspase-1 (1:1000; Zen-bio, China), cleaved Caspase-1 (1:1000; Abcam, UK), cleaved IL-1β (1:1000; Affinity, China), N terminal of GSDMD (1:1000; Abcam, UK), Bcl-2 (1:1000; Proteintech Group, USA) at 4^{o}C overnight. The GADPH (1:5000; Proteintech Group, USA) was probed as internal reference. Alkaline phosphatase-conjugated goat anti-mouse antibody (1:5000; Proteintech Group, USA) and goat anti-rabbit antibody (1:5000; Proteintech Group, USA) were used as secondary antibodies, and incubated at room temperature for 1 h. The protein bands were detected by using an ECL kit (MERCK MILLIOPORE, Germany).

Statistical analysis

Statistical analysis related to bioinformatics was conducted as described above. Besides, all statistical tests were performed with Prism GraphPad Software (La Jolla, CA). Quantitative data are expressed as mean values ± standard deviation of three independent experiments. At least five biological replicates were used for statistical analysis. The unpaired Student t test or ANOVA were used to determine differences among all groups. Differences were considered significant when *P* values were less than 0.05.

Results

Andrographolide decreased RSV viral load and attenuated inflammation in vitro.

Andrographolide has been found to exert antiviral function over a variety of viruses, but its role on RSV infection has not been reported yet. To clarify whether andrographolide has antiviral effect on RSV, we conducted in vitro experiment using human lung carcinoma epithelial cell line A549. Firstly, we investigated whether andrographolide induced cytotoxicity in A549 cell line and selected appropriate concentrations to conduct in vitro experiment. As shown in Fig. 1A, obvious impact on cell viability was seen in concentration more than 20 μM after 36 h treatment. Therefore, we selected 5μM and 10μM as appropriate concentration to conduct following in vitro experiment. Next, we measured the RSV N gene load both at 24 h and 36 h post-infection. After treatment with andrographolide, RSV viral load was noticeably decreased at 36 h dose-dependently (Fig. 1B). To further elucidate the impact of andrographolide on RSV-induced inflammation in vitro, we measured IL-6 and IL-8 levels in cell supernatants 36 h post-infection. Both cytokine levels were dramatically increased post RSV infection, while andrographolide attenuated them significantly (Fig. 1C and D).

Identification of RSV infection-related genes

To identify RSV regulated cellular genes, RNAseq dataset GSE32139 was downloaded from the Gene Expression Omnibus (GEO) database. As presented in Table 2, there were a total of 1519 DEGs between the mock-infected and the RSV group, and among them, 891 were up-regulated, while 628 were down-regulated. The results are presented as heatmap of all DEGs (Fig. 2A), and volcano plot (Fig. 2B). DEGs represented in red were up-regulated, while those in blue were down-regulated. Detail information about

the DEGs of RSV infection was presented as supplementary material (Supplementary Materials Table S1).

Table 2
RSV infection DEGs in GSE32139

Compare	All	Up	Down	Threshold
RSV vs Mock	1519	891	628	DESeq2 pvalue<0.05 |log2FoldChange|>0.5

Andrographolide-related target identification via PharmMapper database

PharmMapper Database and PubChem were used as described in the Materials and Methods. The chemical structure of andrographolide (Fig. 3A) and the potential targets of andrographolide along with their gene symbols are presented in Supplementary Table S2.

GO and KEGG pathway enrichment analysis

As illustrated in Fig. 3B, RSV infection-related genes and andrographolide target genes were merged, and the intersection of the two sets was considered as the potential targets of andrographolide for the treatment of RSV infection. There were 25 genes in total, as presented in Table 3. To further understand these targets, GO and KEGG enrichment analysis were performed and shown in Fig. 3C and D. The top five significant functions were regulation of cytokine-mediated signaling pathway, regulation of response to cytokine stimulus, cellular response to interferon-gamma (IFN-γ), regulation of response to IFN-γ, and regulation of IFN-γ-mediated signaling pathway. The KEGG pathways involved were influenza A, pyruvate metabolism, necroptosis, steroid hormone biosynthesis, NOD-like receptor signaling pathway, cytosolic DNA-sensing pathway, chemokine signaling pathway, prolactin signaling pathway, Leishmaniasis, lipid and atherosclerosis, Coronavirus disease COVID-19, PD-L1 expression and PD-1 checkpoint pathway in cancer, Th1 and Th2 cell differentiation, Toll-like receptor signaling pathway, C-type lectin receptor signaling pathway, Th17 cell differentiation, toxoplasmosis, growth hormone synthesis secretion and action, and 2-Oxocarboxylic acid metabolism. Target genes related to these pathways are listed in Table 4.

Table 3
Potential targets of andrographolide for the treatment of RSV infection

Target gene	Target protein
ADH1C	Alcohol dehydrogenase 1C
AMY1A	Alpha-amylase 1A
ANXA5	Annexin A5
BCAT2	Branched-chain-amino-acid aminotransferase, mitochondrial
CASP1	Caspase-1
CCL5	C-C motif chemokine 5
CFD	Complement factor D
DUSP6	Dual specificity protein phosphatase 6
GLO1	Lactoylglutathione lyase
GMPR	GMP reductase 1
HNMT	Histamine N-methyltransferase
JAK2	Tyrosine-protein kinase JAK2
LTA4H	Leukotriene A-4 hydrolase
MMP12	Macrophage metalloelastase
MMP13	Collagenase 3
NR1H3	Oxysterols receptor LXR-alpha
SEC14L1	SEC14-like protein 1
SORD	Sorbitol dehydrogenase
SPARC	SPARC
STAT1	Signal transducer and activator of transcription 1-alpha/beta
STS	Steryl-sulfatase
SULT1E1	Sulfotransferase Family 1E Member 1
TNNC1	Troponin C, slow skeletal and cardiac muscles
TTR	Transthyretin
TYMS	Thymidylate synthase

Table 4
Target genes involved in KEGG pathways

ID	KEGG Pathway	*P* value	Gene Symbol
hsa05164	Influenza A	0.000886596	CASP1/CCL5/JAK2/STAT1
hsa00620	Pyruvate metabolism	0.006454215	ADH1C/GLO1
hsa04217	Necroptosis	0.007619001	CASP1/JAK2/STAT1
hsa00140	Steroid hormone biosynthesis	0.010690573	STS/SULT1E1
hsa04621	NOD-like receptor signaling pathway	0.011355888	CASP1/CCL5/STAT1
hsa04623	Cytosolic DNA-sensing pathway	0.011373674	CASP1/CCL5
hsa04062	Chemokine signaling pathway	0.01274064	CCL5/JAK2/STAT1
hsa04917	Prolactin signaling pathway	0.013911961	JAK2/STAT1
hsa05140	Leishmaniasis	0.016673315	JAK2/STAT1
hsa05417	Lipid and atherosclerosis	0.017247702	CASP1/CCL5/JAK2
hsa05171	Coronavirus disease - COVID-19	0.021089305	CASP1/CFD/STAT1
hsa05235	PD-L1 expression and PD-1 checkpoint pathway in cancer	0.021902894	JAK2/STAT1
hsa04658	Th1 and Th2 cell differentiation	0.023304382	JAK2/STAT1
hsa04933	AGE-RAGE signaling pathway in diabetic complications	0.027218185	JAK2/STAT1
hsa04620	Toll-like receptor signaling pathway	0.029268752	CCL5/STAT1
hsa04625	C-type lectin receptor signaling pathway	0.029268752	CASP1/STAT1
hsa04659	Th17 cell differentiation	0.031379942	JAK2/STAT1
hsa05145	Toxoplasmosis	0.03355041	JAK2/STAT1
hsa04935	Growth hormone synthesis secretion and action	0.037487397	JAK2/STAT1
hsa01210	2-Oxocarboxylic acid metabolism	0.048190537	BCAT2

RT-qPCR verification of potential target genes

To verify change of gene mRNA expression analyzed by network pharmacology, we extracted total RNA at 24 and 36 h post RSV infection on A594 cells. The expression level of target genes (CASP1/CCL5/JAK2/STAT1) and the downstream gene of CASP1 (which also functions as IL-1β-converting enzyme) were measured using RT-qPCR. As shown in Fig. 4, RSV infection dramatically elevated the expression of CASP1, CCL5, JAK2, STAT1 and IL-1β both at 24 and 36 h. Furthermore,

andrographolide clearly mitigated the increase of CASP1, CCL5, JAK2, STAT1 and IL-1β mRNA levels at 36 h.

Andrographolide inhibited apoptosis of RSV-infected epithelial cells

There are three major programmed cell death pathways, namely, apoptosis, pyroptosis and necroptosis, which have been documented to be involved in airway epithelial cells infected with viruses[35]. Airway epithelial cell death caused by viral infection has been considered an important defense mechanism that restricts virus replication and spread[18]. Since CASP1 is an important gene involved in pyroptosis signal pathway[41], we conducted flow cytometry analysis using Annexin V-FITC/PI dual staining to figure out whether andrographolide have effect on cell death after RSV infection. A549 cells, intervened or not with andrographolide, were collected after 36h infection with RSV, and was stained with Annexin V-FITC/PI according to the manufacturer's instruction. We defined Annexin V positive, PI negative quadrant as early apoptotic cells, while dual Annexin V and PI positive quadrant as late apoptotic or necrotic cells[46]. After 36 h of infection, RSV noticeably increased the ratio of apoptosis of A549 cells. Andrographolide obviously inhibited apoptotic ratio of RSV-infected cells, which was dose-dependent responsive. Similar effect was not seen in uninfected cells (Fig. 5).

Andrographolide elevated protein levels of caspase-1, cleaved caspase-1, N terminal of GSDMD and Bcl-2 to suppress apoptosis and promote pyroptosis of RSV infected cells

As the results of RT-qPCR and flow cytometry had indicated, andrographolide may have impact on death pattern of airway epithelial cells infected with RSV. In the process of pyroptosis, formation of inflammasome cleaves pro-caspase-1 into its active form, which then cleaves Gasdermin-D (GSDMD), pro-IL-1β, pro-IL-18, and pro-IL-33 into biologically active forms[15], resulting the production of IL-1β, IL-33, IL-18 and pyroptosis[28, 40]. Therefore, we measured the protein levels of pro-caspase-1, cleaved caspase-1, cleaved IL-1β and N terminal of GSDMD at 36 h post RSV infection to further elucidate the effects of andrographolide on pyroptosis. The results showed that RSV infection decreased the protein levels of all four, but andrographolide elevated them (Fig. 6). Since B-cell lymphoma-2 (Bcl-2) family play a pivotal role in regulating cell apoptosis, we also assessed the expression level of antiapoptotic protein Bcl-2 to identify the effects of andrographolide on apoptosis. RSV suppressed the expression of antiapoptotic protein Bcl-2 at 36 h post infection, while andrographolide increased it (Fig. 6). Based on the above results, we hypothesized that andrographolide elevated protein levels of caspase-1, cleaved caspase-1, N terminal of GSDMD and Bcl-2 to suppress apoptosis and promote pyroptosis of RSV infected cells.

Discussion

In this study, we discovered that andrographolide decreased RSV viral load and attenuated inflammation in vitro. By using online databases to reveal the RSV infection-related genes and the potential targets of andrographolide, we then verified the change of potential target genes in infection studies in vitro. RSV infection strongly elevated the mRNA level of CASP1, CCL5, JAK2 and STAT1, while andrographolide suppressed the increase of them. Moreover, IL-1β, which is activated by CASP1-mediated cleavage, was

also enormously up-regulated after RSV infection and conspicuously down-regulated by andrographolide at 36 h. Next, we conducted Annexin V-FITC/PI dual staining and Western blot analysis of pivotal proteins involved in apoptosis and pyroptosis to figure out whether andrographolide has influence on death pattern of RSV-infected A549 cells. We found that andrographolide inhibited apoptosis but promoted pyroptosis of infected cells via elevating the protein levels of caspase-1, cleaved caspase-1, N terminal of GSDMD and Bcl-2, indicating that andrographolide might switch the death pattern of RSV-infected cells from apoptosis to pyroptosis. Therefore, we speculated that andrographolide may decreased RSV viral load and attenuated inflammation due to the suppression of apoptosis and promotion of pyroptosis. As far as we known, this is the first time andrographolide was proved to have effect on cell death pattern after RSV infection.

As indicated earlier, andrographolide has attracted much attention and been extensively studied due to its antivirus property. Plenty of studies have shown potential therapeutic properties against numerous viruses[20]. One study indicated that andrographolide's anti-H1N1 virus effects might be related to its inhibition of viral-induced activation of the RLRs signaling pathway[52]. As for EV-D68, Andrographolide inhibits acidification of the virus-containing endocytic vesicle and significantly decreases viral RNA replication and protein synthesis[47]. Despite the wide clinical application of andrographolide in viral infection, there is no relevant research on its effects on RSV infection so far. We conducted in vitro RSV infection model using A549 cell line, assessed andrographolide's antiviral effect via detection of RSV N gene load and pro-inflammatory cytokine levels in cell supernatant, and identified andrographolide decreased RSV viral load and attenuated inflammation in vitro.

By using a network pharmacology approach, we speculated that cell death pattern might be participated in the underlying anti-RSV mechanism of andrographolide. Airway epithelial cell death caused by viral infection has been considered an important defense mechanism that restricts virus replication and spread[18]. There are three major programmed cell death pathways, namely, apoptosis, pyroptosis and necroptosis, which have been documented to be involved in airway epithelial cells infected with viruses[35]. Studies have shown that RSV non-structural proteins (NS1 and NS2) can inhibit pro-apoptotic proteins and promote anti-apoptotic proteins synthesis, which interferes with host cell apoptosis at the early phase of infection, allowing the virus to complete replication[44]. However, at the late phase of infection, the expression of RSV F protein can activate the phosphorylation of p53, leading to transcription of pro-apoptotic proteins and caspase activation, which results in apoptosis of epithelial cells and spread of virus [11]. It has been proposed that apoptosis of infected airway epithelial cells cannot effectively restrict the replication of RSV and may help the virus spread into extrapulmonary organs of the host [12]. Pyroptosis, another major programmed cell death pathway, is a primary cellular response following the sensing of potentially damaging insults, including pathogen ligands, DAMPs, altered levels of host metabolites and environmental irritants[31], and results in the lysis of the affected cells. Recent studies have provided evidence that pyroptosis occurs in vivo, and that it is a potent mechanism used to clear intracellular pathogens[29, 32] and *Shigella flexneri* was reported to inhibit pyroptosis to evade anti-Shigella humoral immunity[24].

In our study, RSV mitigated the antiapoptotic protein Bcl-2 expression to promote apoptosis, and decreased the expression of caspase-1, cleaved caspase-1 and N terminal of GSDMD to inhibit pyroptosis in A549 cells at 36 h post infection. While andrographolide elevated protein levels of those four to suppress apoptosis and promote pyroptosis of RSV infected cells. Several studies have reported that RSV infection induced the expression of antiapoptotic proteins Bcl-2[26, 34, 50], which is consistent with our finding, indicating the suppression effect of RSV infection on cell apoptosis. Andrographolide was reported to exhibit anti-apoptotic potential through the activation of the Akt-BAD pathway in HUVECs during growth factor (GF) deprivation-induced apoptosis[7]. It was also shown to inhibit renal tubular cell apoptosis[27], cardiac apoptosis[25], and regulate the apoptosis-NETosis balance of neutrophils to ameliorate Rheumatoid Arthritis[23]. Recently, study on Enterovirus 71 (EV71) infection had shown similar effect that it inhibited EV71-induced RD cells apoptosis[6].

Although pyroptosis is highly important for an effective antiviral response[3], it can also contribute to the immunopathology and excessive inflammation[16, 37]. The main pathological effect of RSV infection is excessive inflammatory response and tissue damage[45]. Among many pro-inflammatory cytokines released after RSV infection, such as those of the IL-1 family, IL-6, and tumor necrosis factor (TNF-α), IL-1β acts as a predominant pro-inflammatory factor[8, 39]. However, in our study, the mRNA expression levels of caspase-1 and IL-1β decreased after andrographolide treatment. We speculated that andrographolide may exert a negative feedback regulation after inducing pyroptosis to promote virus clearance and restricts the replication of the virus, so as to avoid the excessive synthesis of caspase-1 and IL-1β that would otherwise cause excessive inflammation.

Nevertheless, there were some obvious limitations in our study, which still need improvement. First, our experiments were performed in vitro, and therefore, the effects require in vivo confirmation. Second, a detailed molecular mechanism of how andrographolide affects the apoptosis and pyroptotosis in RSV infection, remains to be fully elucidated. Clearly, further experiments should be conducted to investigate how andrographolide influences the death pattern of RSV-infected airway epithelial cell and how it translates into ameliorating the pathology in an animal model for eventual clinical applications.

Declarations

Acknowledgements

This work was supported by National Natural Science Foundation of China (81800009) and The Open Project of State Key Laboratory of Innovative Natural Medicine and TCM Injections (QFSKL2020020).

Author contributions

All authors contributed to the study conception and design. SC performed the experiments, data analysis and manuscript draft. JL performed the bioinformatics data analysis. EL and JX critically revised the manuscript. All authors read and approved the final manuscript

Conflict of interest

The authors declare they have no conflict of interests.

Ethical approval

This article does not contain any studies with human participants or animals performed by any of the authors.

References

1. Banerjee S, Kar A, Mukherjee P, Haldar P, Sharma N, Katiyar C (2021) Immunoprotective potential of Ayurvedic herb Kalmegh (Andrographis paniculata) against respiratory viral infections - LC-MS/MS and network pharmacology analysis. Phytochem Anal 32:629–639. http://dx.doi.org/10.1002/pca.3011
2. Battles M, McLellan J (2019) Respiratory syncytial virus entry and how to block it. Nat Rev Microbiol 17:233–245. http://dx.doi.org/10.1038/s41579-019-0149-x
3. Carty M, Guy C, Bowie AG (2021) Detection of Viral Infections by Innate Immunity. Biochem Pharmacol. 183:114316.http://dx.doi.org/10.1016/j.bcp.2020.114316
4. CHAKRAVARTI R, CHAKRAVARTI D (1951) Andrographolide, the active constituent of Andrographis paniculata Nees; a preliminary communication. The Indian medical gazette 86:96–97.http://dx.doi.org/
5. Chao WW, Lin BF (2010) Isolation and identification of bioactive compounds in Andrographis paniculata (Chuanxinlian). Chin Med 5:17. http://dx.doi.org/10.1186/1749-8546-5-17
6. Chao WW, Kuo YH, Lin BF (2021) Isolation and Identification of Andrographis paniculata (Chuanxinlian) and Its Biologically Active Constituents Inhibited Enterovirus 71-Induced Cell Apoptosis. Front Pharmacol 12:762285. http://dx.doi.org/10.3389/fphar.2021.762285
7. Chen J, Hsiao G, Lee A, Wu C, Yen M (2004) Andrographolide suppresses endothelial cell apoptosis via activation of phosphatidyl inositol-3-kinase/Akt pathway. Biochem Pharmacol 67:1337–1345. http://dx.doi.org/10.1016/j.bcp.2003.12.015
8. Choudhury S, Ma X, Abdullah S, Zheng H (2021) Activation and Inhibition of the NLRP3 Inflammasome by RNA Viruses. J Inflamm Res 14:1145–1163. http://dx.doi.org/10.2147/jir.S295706
9. Deng Y, Chen W, Zang N, Li S, Luo Y, Ni K, Wang L, Xie X, Liu W, Yang X, Fu Z, Liu E (2011) The antiasthma effect of neonatal BCG vaccination does not depend on the Th17/Th1 but IL-17/IFN-γ balance in a BALB/c mouse asthma model. J Clin Immunol 31:419–429. http://dx.doi.org/10.1007/s10875-010-9503-5
10. Ding Y, Chen L, Wu W, Yang J, Yang Z, Liu S (2017) Andrographolide inhibits influenza A virus-induced inflammation in a murine model through NF-κB and JAK-STAT signaling pathway. Microbes Infect 19:605–615. http://dx.doi.org/10.1016/j.micinf.2017.08.009

11. Eckardt-Michel J, Lorek M, Baxmann D, Grunwald T, Keil G, Zimmer G (2008) The fusion protein of respiratory syncytial virus triggers p53-dependent apoptosis. J Virol 82:3236–3249. http://dx.doi.org/10.1128/jvi.01887-07
12. Eisenhut M (2006) Extrapulmonary manifestations of severe respiratory syncytial virus infection–a systematic review. Crit Care (London England) 10:R107. http://dx.doi.org/10.1186/cc4984
13. Elasoru S, Rhana P, de Oliveira Barreto T, Naves de Souza D, Menezes-Filho J, Souza D, Loes Moreira M, Gomes Campos M, Adedosu O, Roman-Campos D, Melo M, Cruz J (2021) Andrographolide protects against isoproterenol-induced myocardial infarction in rats through inhibition of L-type Ca and increase of cardiac transient outward K currents. Eur J Pharmacol 906:174194. http://dx.doi.org/10.1016/j.ejphar.2021.174194
14. Gias E, Nielsen SU, Morgan LA, Toms GL (2008) Purification of human respiratory syncytial virus by ultracentrifugation in iodixanol density gradient. J Virol Methods 147:328–332. http://dx.doi.org/10.1016/j.jviromet.2007.09.013
15. He Y, Hara H, Núñez G (2016) Mechanism and Regulation of NLRP3 Inflammasome Activation. Trends Biochem Sci 41:1012–1021. http://dx.doi.org/10.1016/j.tibs.2016.09.002
16. He Z, Chen J, Zhu X, An S, Dong X, Yu J, Zhang S, Wu Y, Li G, Zhang Y, Wu J, Li M (2018) NLRP3 Inflammasome Activation Mediates Zika Virus-Associated Inflammation. J Infect Dis 217:1942–1951. http://dx.doi.org/10.1093/infdis/jiy129
17. Hopkins A (2008) Network pharmacology: the next paradigm in drug discovery. Nat Chem Biol 4:682–690. http://dx.doi.org/10.1038/nchembio.118
18. Imre G (2020) Cell death signalling in virus infection. Cell Signal 76:109772. http://dx.doi.org/10.1016/j.cellsig.2020.109772
19. Kumar S, Singh B, Bajpai V (2021) Andrographis paniculata (Burm.f.) Nees: Traditional uses, phytochemistry, pharmacological properties and quality control/quality assurance. J Ethnopharmacol 275:114054. http://dx.doi.org/10.1016/j.jep.2021.114054
20. Latif R, Wang CY (2020) Andrographolide as a potent and promising antiviral agent. Chin J Nat Med 18:760–769. http://dx.doi.org/10.1016/s1875-5364(20)60016-4
21. Li B, Li Z, Liu M, Tian J, Cui Q (2021) Progress in Traditional Chinese Medicine Against Respiratory Viruses: A Review. Front Pharmacol 12:743623. http://dx.doi.org/10.3389/fphar.2021.743623
22. Li F, Lee E, Sun X, Wang D, Tang H, Zhou G (2020) Design, synthesis and discovery of andrographolide derivatives against Zika virus infection. Eur J Med Chem 187:111925. http://dx.doi.org/10.1016/j.ejmech.2019.111925
23. Li X, Yuan K, Zhu Q, Lu Q, Jiang H, Zhu M, Huang G, Xu A (2019) Andrographolide Ameliorates Rheumatoid Arthritis by Regulating the Apoptosis-NETosis Balance of Neutrophils. International journal of molecular sciences 2010.3390/ijms20205035
24. Li Z, Liu W, Fu J, Cheng S, Xu Y, Wang Z, Liu X, Shi X, Liu Y, Qi X, Liu X, Ding J, Shao F (2021) Shigella evades pyroptosis by arginine ADP-riboxanation of caspase-11. Nature10.1038/s41586-021-04020-1

25. Lin K, Marthandam Asokan S, Kuo W, Hsieh Y, Lii C, Viswanadha V, Lin Y, Wang S, Yang C, Huang C (2020) Andrographolide mitigates cardiac apoptosis to provide cardio-protection in high-fat-diet-induced obese mice. Environ Toxicol 35:707–713. http://dx.doi.org/10.1002/tox.22906
26. Lindemans CA, Coffer PJ, Schellens IM, de Graaff PM, Kimpen JL, Koenderman L (2006) Respiratory syncytial virus inhibits granulocyte apoptosis through a phosphatidylinositol 3-kinase and NF-kappaB-dependent mechanism. J Immunol 176:5529–5537. http://dx.doi.org/10.4049/jimmunol.176.9.5529
27. Liu W, Liang L, Zhang Q, Li Y, Yan S, Tang T, Ren Y, Mo J, Liu F, Chen X, Lan T (2021) Effects of andrographolide on renal tubulointersticial injury and fibrosis. Evidence of its mechanism of action. Phytomedicine: Int J phytotherapy phytopharmacology 91:153650. http://dx.doi.org/10.1016/j.phymed.2021.153650
28. Malinczak C, Schuler C, Duran A, Rasky A, Mire M, Núñez G, Lukacs N, Fonseca W (2021) NLRP3-Inflammasome Inhibition during Respiratory Virus Infection Abrogates Lung Immunopathology and Long-Term Airway Disease Development. Viruses 1310.3390/v13040692
29. Maltez V, Tubbs A, Cook K, Aachoui Y, Falcone E, Holland S, Whitmire J, Miao E (2015) Inflammasomes Coordinate Pyroptosis and Natural Killer Cell Cytotoxicity to Clear Infection by a Ubiquitous Environmental Bacterium. Immunity 43:987–997. http://dx.doi.org/10.1016/j.immuni.2015.10.010
30. McKimm-Breschkin JL (2004) A simplified plaque assay for respiratory syncytial virus–direct visualization of plaques without immunostaining. J Virol Methods 120:113–117. http://dx.doi.org/10.1016/j.jviromet.2004.02.020
31. Miao E, Rajan J, Aderem A (2011) Caspase-1-induced pyroptotic cell death. Immunol Rev 243:206–214. http://dx.doi.org/10.1111/j.1600-065X.2011.01044.x
32. Miao EA, Leaf IA, Treuting PM, Mao DP, Dors M, Sarkar A, Warren SE, Wewers MD, Aderem A (2010) Caspase-1-induced pyroptosis is an innate immune effector mechanism against intracellular bacteria. Nat Immunol 11:1136–1142. http://dx.doi.org/10.1038/ni.1960
33. Mooney K, Melvin M, Douglas T (2014) Ribavirin: the need for exposure precautions. Clin J Oncol Nurs 18:E93. 96.http://dx.doi.org/10.1188/14.Cjon.E93-e96
34. Nakamura-López Y, Villegas-Sepúlveda N, Sarmiento-Silva RE, Gómez B (2011) Intrinsic apoptotic pathway is subverted in mouse macrophages persistently infected by RSV. Virus Res 158:98–107. http://dx.doi.org/10.1016/j.virusres.2011.03.016
35. Paolini A, Borella R, De Biasi S, Neroni A, Mattioli M, Lo Tartaro D, Simonini C, Franceschini L, Cicco G, Piparo A, Cossarizza A, Gibellini L (2021) Cell Death in Coronavirus Infections: Uncovering Its Role during COVID-19. Cells 1010.3390/cells10071585
36. Restori K, Srinivasa B, Ward B, Fixman E (2018) Neonatal Immunity, Respiratory Virus Infections, and the Development of Asthma. Front Immunol 9:1249. http://dx.doi.org/10.3389/fimmu.2018.01249
37. Rodrigues TS, de Sá KSG, Ishimoto AY, Becerra A, Oliveira S, Almeida L, Gonçalves AV, Perucello DB, Andrade WA, Castro R, Veras FP, Toller-Kawahisa JE, Nascimento DC, de Lima MHF, Silva CMS,

Caetite DB, Martins RB, Castro IA, Pontelli MC, de Barros FC, do Amaral NB, Giannini MC, Bonjorno LP, Lopes MIF, Santana RC, Vilar FC, Auxiliadora-Martins M, Luppino-Assad R, de Almeida SCL, de Oliveira FR, Batah SS, Siyuan L, Benatti MN, Cunha TM, Alves-Filho JC, Cunha FQ, Cunha LD, Frantz FG, Kohlsdorf T, Fabro AT, Arruda E, de Oliveira RDR, Louzada-Junior P, Zamboni DS (2021) Inflammasomes are activated in response to SARS-CoV-2 infection and are associated with COVID-19 severity in patients. J Exp Med 21810.1084/jem.20201707

38. Sareer O, Ahmad S, Umar S (2014) Andrographis paniculata: a critical appraisal of extraction, isolation and quantification of andrographolide and other active constituents. Nat Prod Res 28:2081–2101. http://dx.doi.org/10.1080/14786419.2014.924004
39. Schuler C, Malinczak C, Best S, Morris S, Rasky A, Ptaschinski C, Lukacs N, Fonseca W (2020) Inhibition of uric acid or IL-1β ameliorates respiratory syncytial virus immunopathology and development of asthma. Allergy 75:2279–2293. http://dx.doi.org/10.1111/all.14310
40. Shen C, Zhang Z, Xie T, Ji J, Xu J, Lin L, Yan J, Kang A, Dai Q, Dong Y, Shan J, Wang S, Zhao X (2019) Rhein Suppresses Lung Inflammatory Injury Induced by Human Respiratory Syncytial Virus Through Inhibiting NLRP3 Inflammasome Activation via NF-κB Pathway in Mice. Front Pharmacol 10:1600. http://dx.doi.org/10.3389/fphar.2019.01600
41. Shi J, Gao W, Shao F (2017) Pyroptosis: Gasdermin-Mediated Programmed Necrotic Cell Death. Trends Biochem Sci 42:245–254. http://dx.doi.org/10.1016/j.tibs.2016.10.004
42. Shi T, McAllister D, O'Brien K, Simoes E, Madhi S, Gessner B, Polack F, Balsells E, Acacio S, Aguayo C, Alassani I, Ali A, Antonio M, Awasthi S, Awori J, Azziz-Baumgartner E, Baggett H, Baillie V, Balmaseda A, Barahona A, Basnet S, Bassat Q, Basualdo W, Bigogo G, Bont L, Breiman R, Brooks W, Broor S, Bruce N, Bruden D, Buchy P, Campbell S, Carosone-Link P, Chadha M, Chipeta J, Chou M, Clara W, Cohen C, de Cuellar E, Dang D, Dash-Yandag B, Deloria-Knoll M, Dherani M, Eap T, Ebruke B, Echavarria M, de Freitas Lázaro Emediato C, Fasce R, Feikin D, Feng L, Gentile A, Gordon A, Goswami D, Goyet S, Groome M, Halasa N, Hirve S, Homaira N, Howie S, Jara J, Jroundi I, Kartasasmita C, Khuri-Bulos N, Kotloff K, Krishnan A, Libster R, Lopez O, Lucero M, Lucion F, Lupisan S, Marcone D, McCracken J, Mejia M, Moisi J, Montgomery J, Moore D, Moraleda C, Moyes J, Munywoki P, Mutyara K, Nicol M, Nokes D, Nymadawa P, da Costa Oliveira M, Oshitani H, Pandey N, Paranhos-Baccalà G, Phillips L, Picot V, Rahman M, Rakoto-Andrianarivelo M, Rasmussen Z, Rath B, Robinson A, Romero C, Russomando G, Salimi V, Sawatwong P, Scheltema N, Schweiger B, Scott J, Seidenberg P, Shen K, Singleton R, Sotomayor V, Strand T, Sutanto A, Sylla M, Tapia M, Thamthitiwat S, Thomas E, Tokarz R, Turner C, Venter M, Waicharoen S, Wang J, Watthanaworawit W, Yoshida L, Yu H, Zar H, Campbell H, Nair H (2017) Global, regional, and national disease burden estimates of acute lower respiratory infections due to respiratory syncytial virus in young children in 2015: a systematic review and modelling study. Lancet (London England) 390:946–958. http://dx.doi.org/10.1016/s0140-6736(17)30938-8
43. Srikanth L, Sarma P (2021) Andrographolide binds to spike glycoprotein and RNA-dependent RNA polymerase (NSP12) of SARS-CoV-2 by in silico approach: a probable molecule in the development

of anti-coronaviral drug. J genetic Eng Biotechnol 19:101. http://dx.doi.org/10.1186/s43141-021-00201-7

44. Thomas K, Monick M, Staber J, Yarovinsky T, Carter A, Hunninghake G (2002) Respiratory syncytial virus inhibits apoptosis and induces NF-kappa B activity through a phosphatidylinositol 3-kinase-dependent pathway. J Biol Chem 277:492–501. http://dx.doi.org/10.1074/jbc.M108107200
45. Vázquez Y, González L, Noguera L, González P, Riedel C, Bertrand P, Bueno S (2019) Cytokines in the Respiratory Airway as Biomarkers of Severity and Prognosis for Respiratory Syncytial Virus Infection: An Update. Front Immunol 10:1154. http://dx.doi.org/10.3389/fimmu.2019.01154
46. Vermes I, Haanen C, Steffens-Nakken H, Reutelingsperger C (1995) A novel assay for apoptosis. Flow cytometric detection of phosphatidylserine expression on early apoptotic cells using fluorescein labelled Annexin V. J Immunol Methods 184:39–51. http://dx.doi.org/10.1016/0022-1759(95)00072-i
47. Wang D, Guo H, Chang J, Wang D, Liu B, Gao P, Wei W (2018) Andrographolide Prevents EV-D68 Replication by Inhibiting the Acidification of Virus-Containing Endocytic Vesicles. Front Microbiol 9:2407. http://dx.doi.org/10.3389/fmicb.2018.02407
48. Wang D, Xiang Y, Wei Z, Yao H, Shen T (2021) Andrographolide and its derivatives are effective compounds for gastrointestinal protection: a review. Eur Rev Med Pharmacol Sci 25:2367–2382. http://dx.doi.org/10.26355/eurrev_202103_25276
49. Wang X, Shen Y, Wang S, Li S, Zhang W, Liu X, Lai L, Pei J, Li H (2017) PharmMapper 2017 update: a web server for potential drug target identification with a comprehensive target pharmacophore database. Nucleic Acids Res 45:W356–W360. http://dx.doi.org/10.1093/nar/gkx374
50. Xiang Z, Liang Z, Yanfeng H, Leitao K (2017) Persistence of RSV promotes proliferation and epithelial-mesenchymal transition of bronchial epithelial cells through Nodal signaling. J Med Microbiol 66:1499–1505. http://dx.doi.org/10.1099/jmm.0.000581
51. Xing Y, Proesmans M (2019) New therapies for acute RSV infections: where are we? Eur J Pediatrics 178:131–138. http://dx.doi.org/10.1007/s00431-018-03310-7
52. Yu B, Dai CQ, Jiang ZY, Li EQ, Chen C, Wu XL, Chen J, Liu Q, Zhao CL, He JX, Ju DH, Chen XY (2014) Andrographolide as an anti-H1N1 drug and the mechanism related to retinoic acid-inducible gene-I-like receptors signaling pathway. Chin J Integr Med 20:540–545. http://dx.doi.org/10.1007/s11655-014-1860-0
53. Zhang H, Li S, Si Y, Xu H (2021) Andrographolide and its derivatives: Current achievements and future perspectives. Eur J Med Chem 224:113710. http://dx.doi.org/10.1016/j.ejmech.2021.113710

Figures

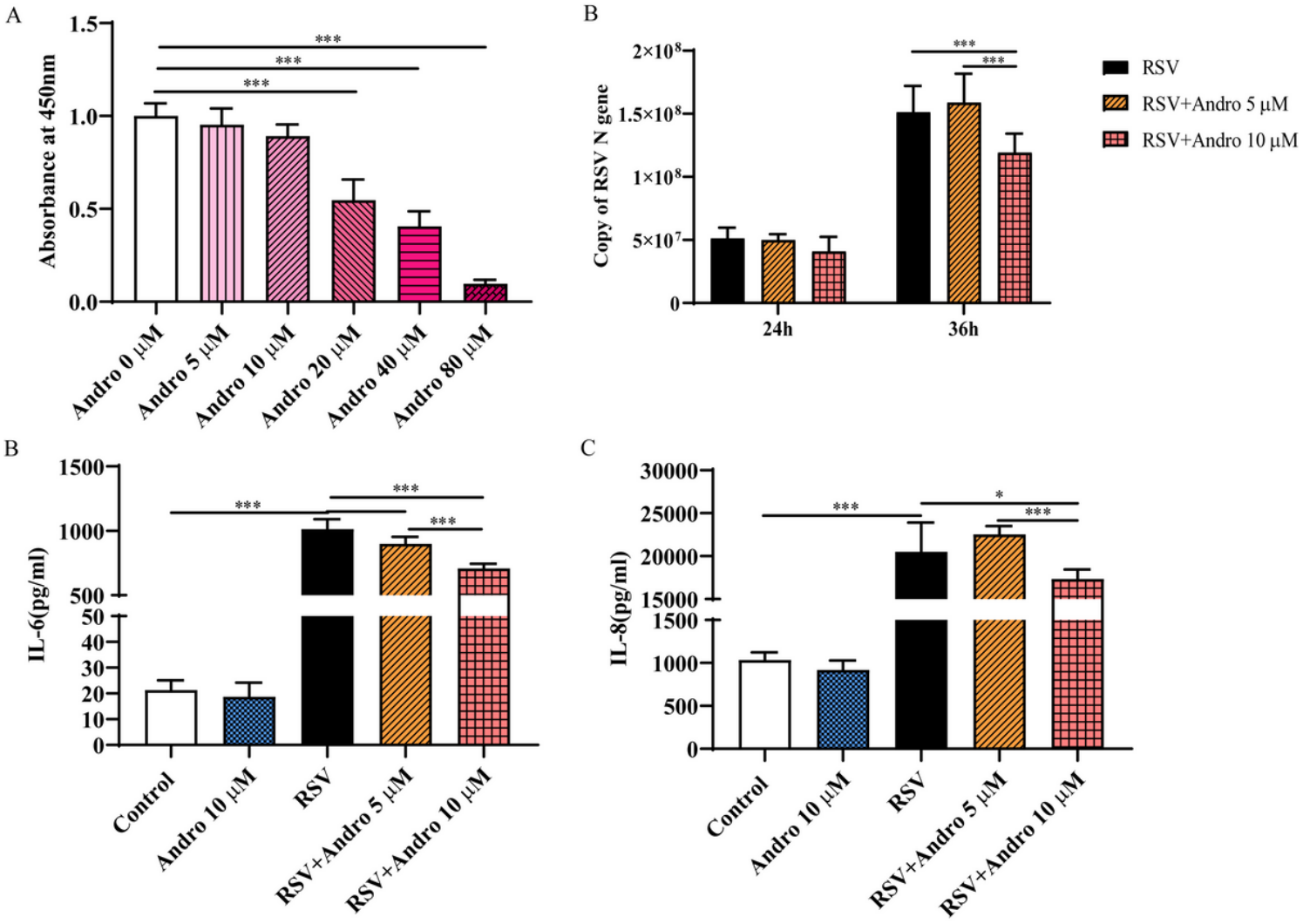

Figure 1

Andrographolide decreased RSV viral load and attenuated inflammation in vitro. (A) Cytotoxicity of andrographolide on A549 cells were tested using CCK-8 kit. After RSV infection (MOI=1), cells were treated with andrographolide (5μM and 10μM) or not for 36 h. (B) Total RNA was extracted to quantify the RSV N gene load. (C) (D) IL-6 and IL-8 levels of cell supernatants were detected. Data were shown as Mean ± SD of three independent experiments (n≥5). Data were analyzed using one-way ANOVA. ***$P <$ 0.005.

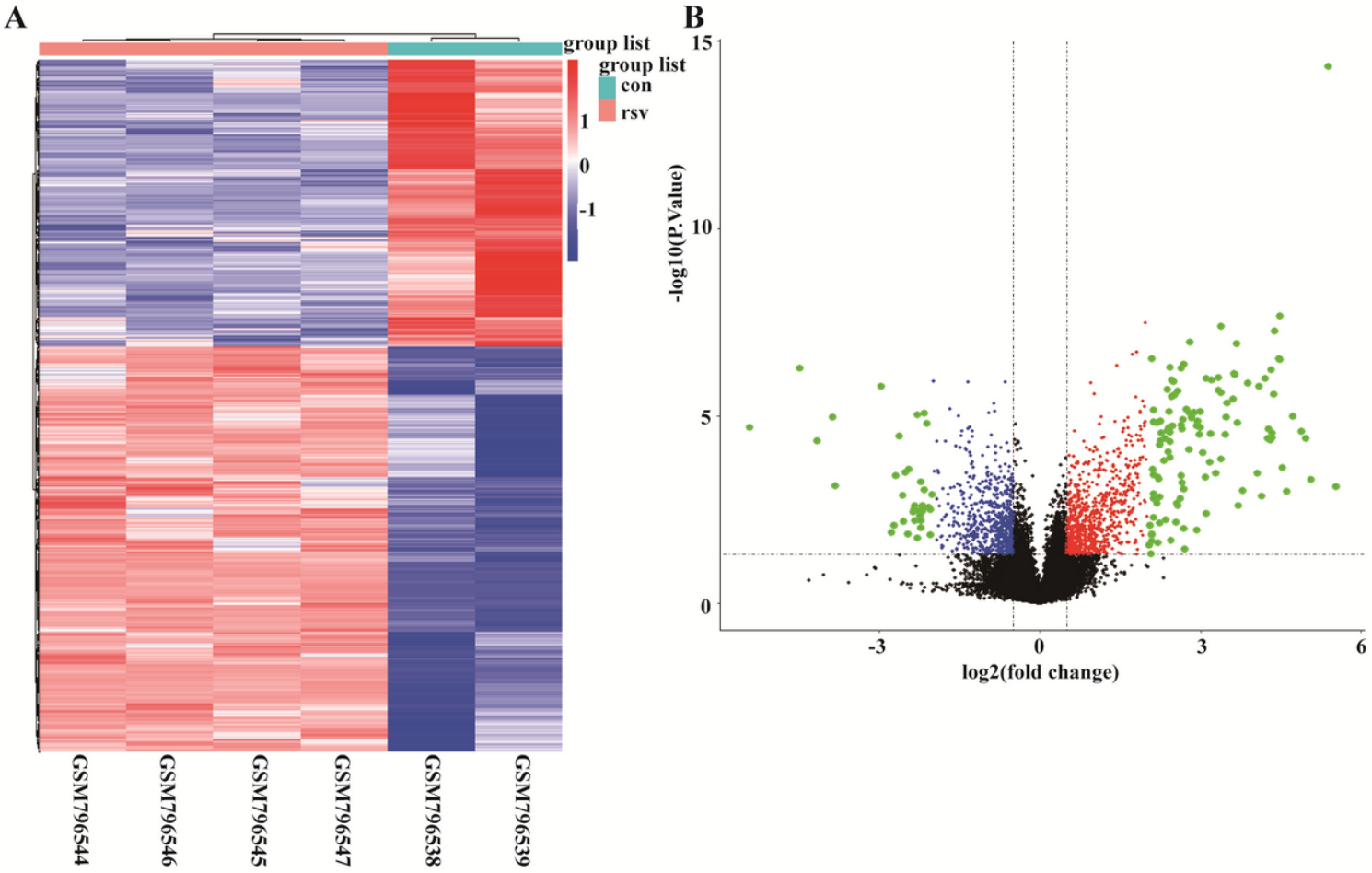

Figure 2

Identification of RSV infection-related genes. RNAseq dataset GSE32139 was downloaded from the Gene Expression Omnibus (GEO) database(https://www.ncbi.nlm.nih.gov/geo/). (A) Heatmap of RSV infection-associated differentially expressed genes (DEGs) analyzed in GSE32139. (B) Volcano plot of RSV infection-associated differentially expressed genes (DEGs) analyzed in GSE32139.

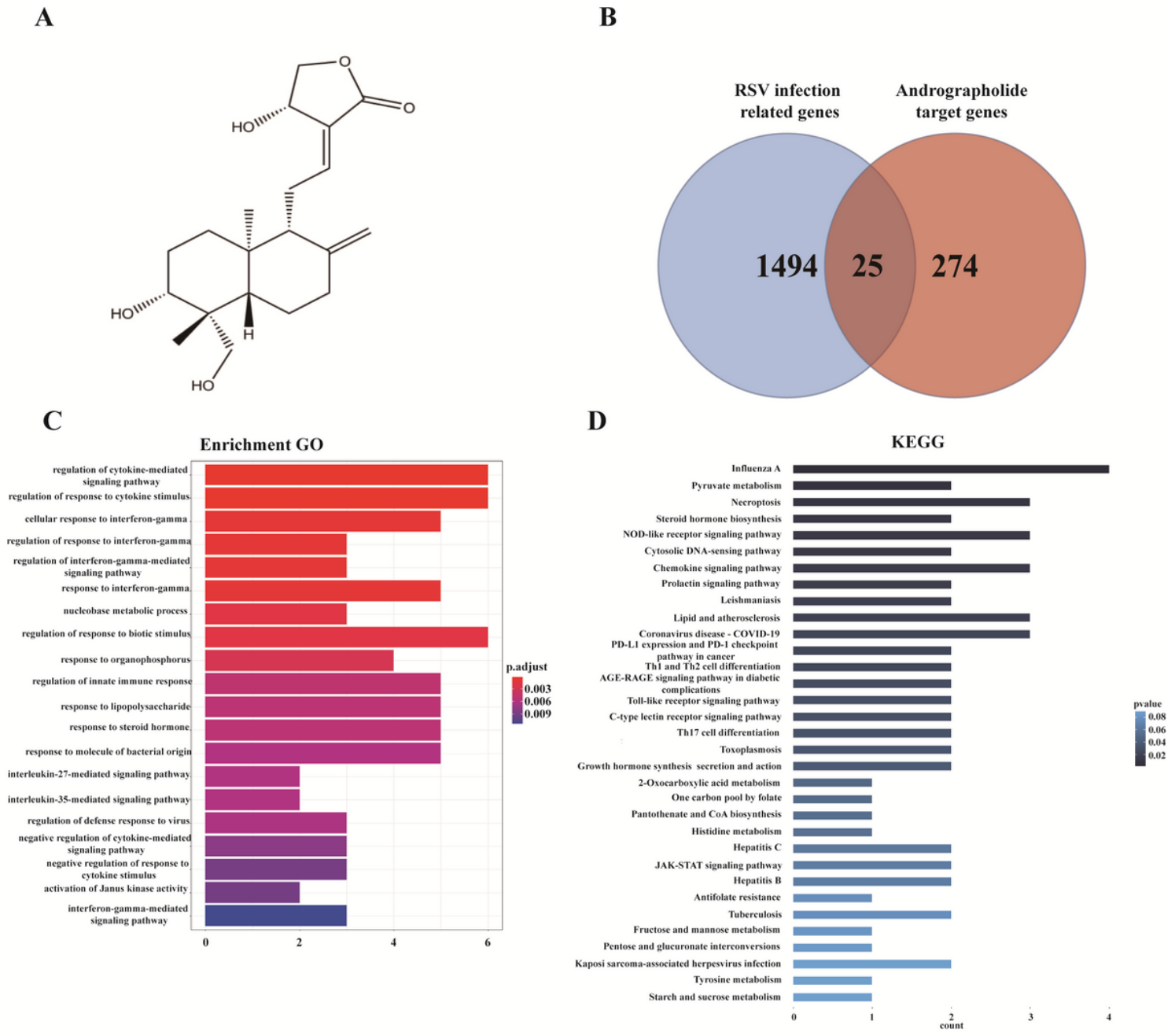

Figure 3

Potential targets of andrographolide for the treatment of RSV infection. PharmMapper Database (http://www.lilab-ecust.cn/pharmmapper/) were used to retrieve the predicted target proteins of Andrographolide. The RSV infection-related and the andrographolide-related genes were merged and the intersection of the two parts was considered as the potential targets of andrographolide for the treatment of RSV infection. (A) Chemical structure of Andrographolide. (B) Venn diagram of potential targets of Andrographolide for RSV infection. (C) GO enrichment analysis of 25 potential target genes. (D) KEGG pathway analysis of 25 potential target genes.

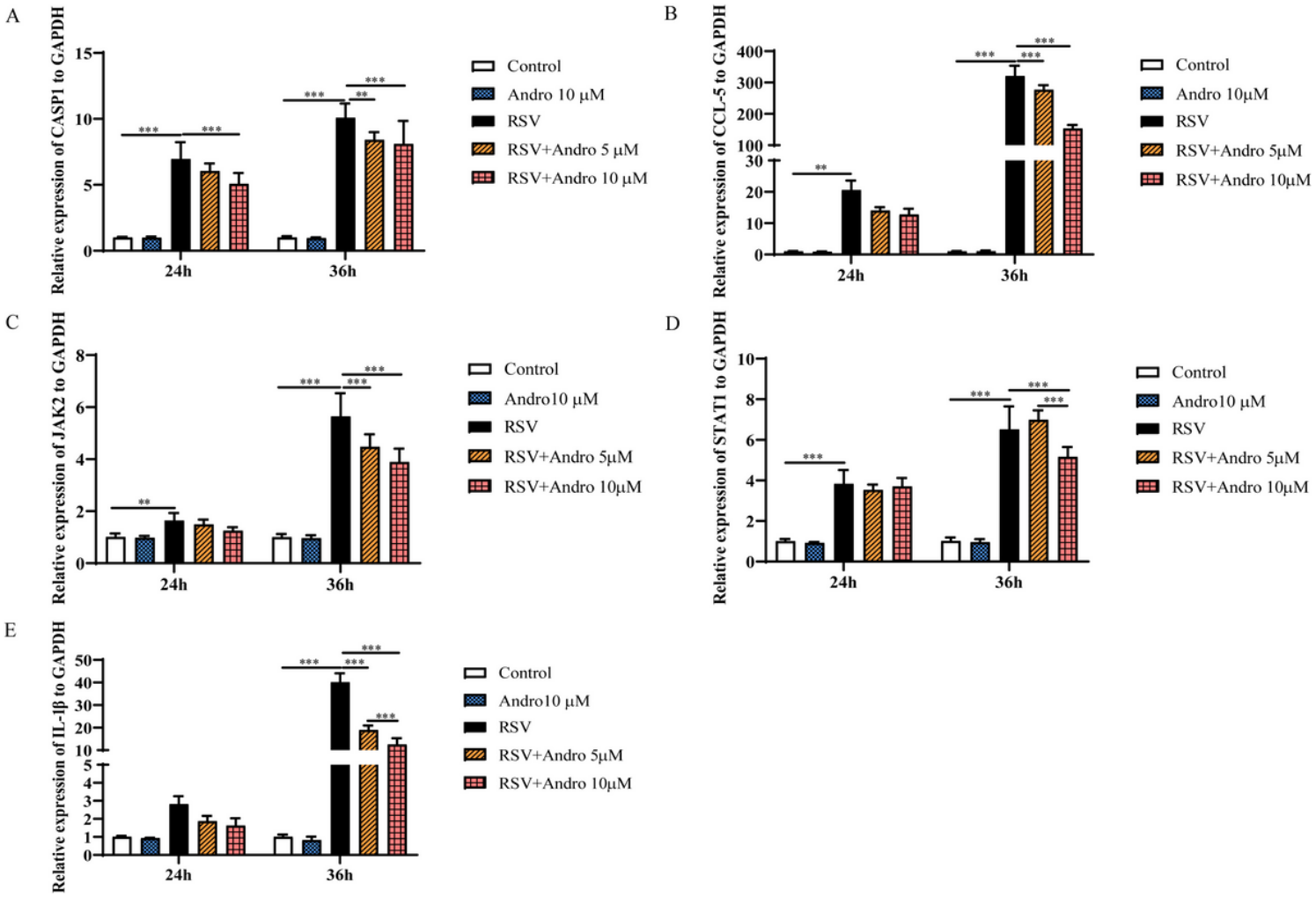

Figure 4

Quantitative real-time polymerase chain reaction verification. Total RNA of A549 cells treated with andrographolide (5μM and 10μM) or not for 24 h and 36 h post RSV infection (MOI=1) were extracted to determine the mRNA expression level of Caspase-1(CASP1), CCL5, JAK2, STAT1 and IL-1β by quantitative real-time PCR. (A)The mRNA expression levels of CASP1. (B) The mRNA expression levels of CCL5. (C) The mRNA expression levels of JAK2. (D) The mRNA expression levels of STAT1. (E) The mRNA expression levels of IL-1β. Data were shown as Mean ± SD of three independent experiments (n≥4). Data were analyzed using one-way ANOVA. *$P < 0.05$, **$P < 0.01$, ***$P < 0.005$.

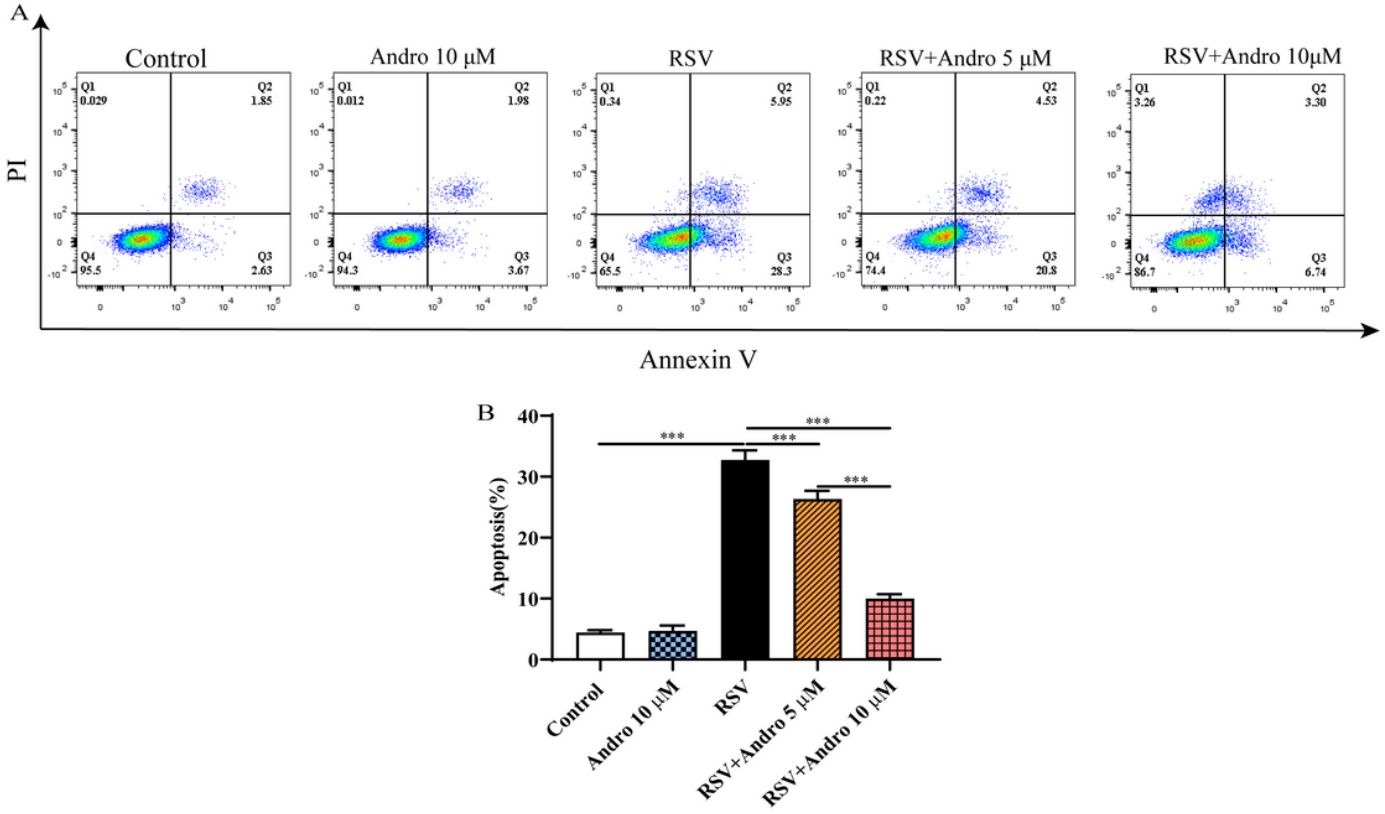

Figure 5

Andrographolide inhibited apoptosis of RSV-infected epithelial cell. (A) A549 cells treated with andrographolide (5μM and 10μM) or not at 36 h post RSV infection (MOI=1) were stained with Annexin V-FITC/PI. (B)Percentage of apoptotic cells were shown(n=6). Data were analyzed using one-way ANOVA. *P < 0.05, **P <0.01, ***P < 0.005.

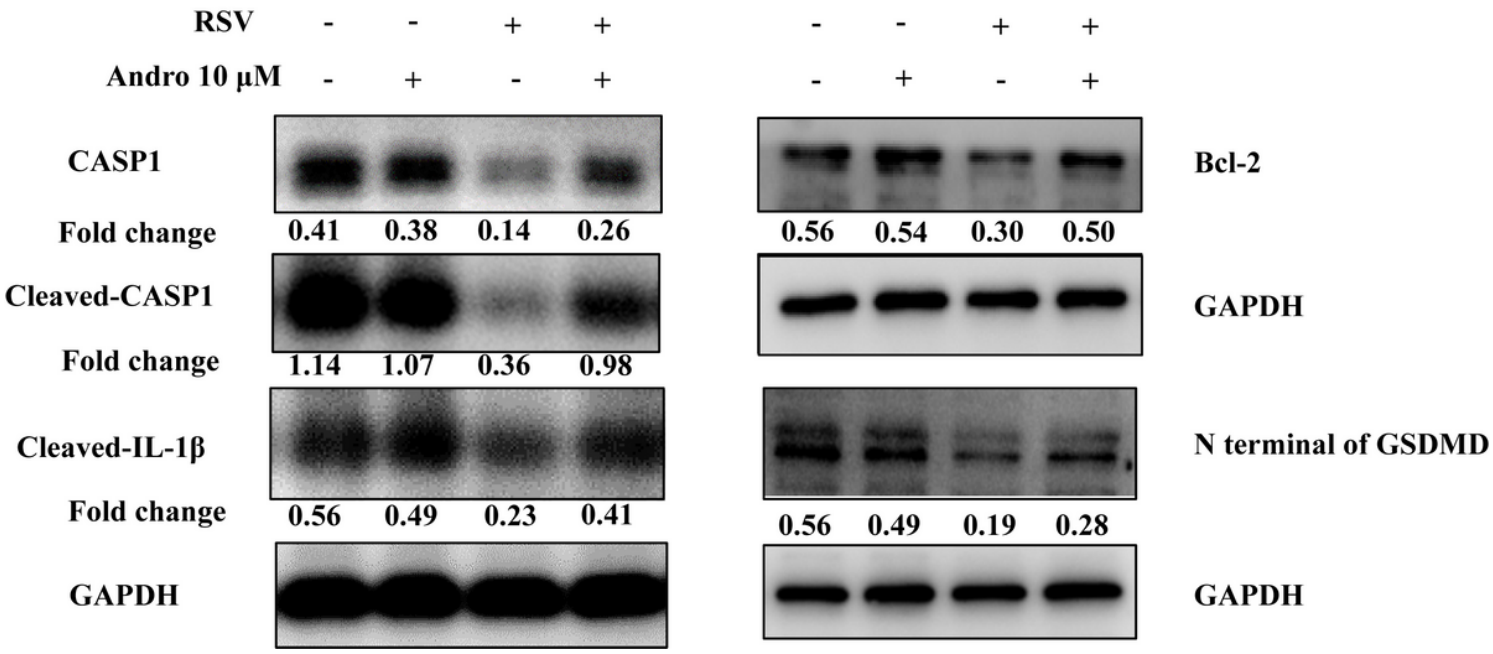

Figure 6

Andrographolide suppressed apoptosis and promoted pyroptosis of RSV infected cells. A549 cells treated with andrographolide (10μM) or not at 36 h post RSV infection (MOI=1) were collected to extract whole protein. Protein levels of caspase-1, cleaved caspase-1 P20, cleaved-IL-1β, Bcl-2, N terminal of GSDMD were determined by Western blotting. GAPDH was determined as reference protein. Fold change of caspase-1, cleaved caspase-1 P20, cleaved IL-1β Bcl-2, N terminal of GSDMD over GAPDH was calculated. Three independent experiments were conducted.

Supplementary Files

This is a list of supplementary files associated with this preprint. Click to download.

- SupplementaryMaterialTableS1.docx
- SupplementaryMaterialTableS2.doc